Ultralow interfacial tensions in water– n -alkane–surfactant systems

T. Sottmann and R. Strey

Citation: The Journal of Chemical Physics **106**, 8606 (1997); doi: 10.1063/1.473916
View online: http://dx.doi.org/10.1063/1.473916
View Table of Contents: http://scitation.aip.org/content/aip/journal/jcp/106/20?ver=pdfcov
Published by the AIP Publishing

Ultralow interfacial tensions in water–*n*-alkane–surfactant systems

T. Sottmann and R. Strey[a),b)]
Max-Planck Institut für Biophysikalische Chemie, Postfach 2841, D-37018 Göttingen, Germany

(Received 6 December 1996; accepted 20 February 1997)

The interfacial tensions between water- and oil-rich phases in the presence of microemulsions have been measured for ternary systems of water, *n*-alkanes, and nonionic alkylpolyglycolether surfactants (C_iE_j). It is found that the minimum of the interfacial tension curve, which is observed for each system in conjunction with the well-known phenomenon of phase inversion, depends sensitively, but systematically, on the chemical nature of the oil and the surfactant. Specifically, the minimum value of the interfacial tension $\overline{\sigma_{ab}}$ decreases by 1 order of magnitude on decreasing either the carbon number of the alkane k by 6, or the number of oxyethylene groups j by 3, or by increasing the number of carbon atoms in the surfactant tail i by 2. The numerical values of the interfacial tensions as a function of temperature are presented along with an empirical description previously suggested [R. Strey, Colloid and Polymer Sci. **272**, 1005 (1994)]. From the analysis, in terms of bending energy one obtains estimates for the bending and saddle-splay constants. The similar shape of the interfacial tension curves permits a superposition of the data for all 19 systems in support of a scaling relation recently derived [S. Leitao, A. M. Somoza, M. M. Telo da Gama, T. Sottmann, and R. Strey, J. Chem. Phys. **105**, 2875 (1996)]. Furthermore, we note a striking coincidence of the numerical values of critical amplitude ratio $R=\sigma_0\xi_0{}^2=0.37$ kT in near-critical systems and the product $\overline{\sigma_{ab}}\overline{\xi^2}=0.44(\pm0.10)$ kT where $\overline{\xi}$ is the maximum length scale in the bicontinuous microemulsions. © *1997 American Institute of Physics.* [S0021-9606(97)50820-8]

I. INTRODUCTION

The interfacial tension between a microemulsion and a water- or oil-rich excess phase is, in general, very low. In the case where the microemulsion coexists simultaneously with a water- and an oil-rich excess phase, the interfacial tension between these latter two phases becomes ultralow. This striking phenomenon is related to the formation and properties of an extended internal interfacial film within the microemulsions. In microemulsions, the surfactant molecules form a saturated, flexible, almost tensionless interfacial film. The surfactant molecules optimize the area occupied within the film until lateral interaction and screening of direct water–oil contact are minimized.[1–6] The curvature of the film within the microemulsion is governed by the geometry of the surfactant molecules in conjunction with their interaction with the solvents. Although the details of the interactions, and concomitantly the interfacial stress profile, are still unknown, their interplay may be phenomenologically summarized by a few parameters that characterize the bending properties of the film.[7] The parameter preferred curvature, c_0, controls the mean curvature. To what extent the actual curvature resembles the preferred curvature depends on the magnitude of the bending constants, κ and $\overline{\kappa}$.

During the past 15 years a number of experimental investigations were devoted to clarifying the origin of the ultralow tensions. Cazabat *et al.*[8] focused on the connection of phase behavior, the critical end-point tensions, and trends with salinity. Kunieda and Shinoda[9] for the first time used the pure nonionic alkylpolyglycolethers and temperature as tuning variable. Schechter *et al.*[10] noticed the relation between solubilization capacity and ultralow tensions for technical grade surfactant systems. Widom[11] suggested discriminating between microemulsions and simple systems by the wetting properties of the middle-phase microemulsions. Fletcher and colleagues[12,13] performed the first systematic variations of oil chain length and surfactant type, including nonionic alkylpolyglycolethers. Kahlweit *et al.*[14] noticed the connection between length scales, properties of the three-phase bodies, and the numerical values of the interfacial tensions. Bonkhoff *et al.*[15] analyzed the interfacial tensions of some ternary nonionic systems in terms of critical scaling relations.

Recently, one of us proposed a simple empirical interfacial tension relation capable of describing the whole temperature range,[16] irrespective of the surfactant being in the lower, $\underline{2}$, in the middle, 3, or the upper phase, $\overline{2}$. The idea advanced was that the film curvature within the microemulsion differs from that of the flat interfacial film in the macroscopic interface, and that this free-energy difference shows up as interfacial tension due to the bending elasticity of the film. More recently, we were able to present evidence that both the phase diagrams[17] and interfacial tensions[18] show striking shape similarities, which led us to postulate the existence of corresponding states for microemulsion systems.[17] Leitao *et al.*[19] showed that Helfrich's bending energy expression[7] needs to be modified if applied to microemulsions. The treatment[16,19] connects in a simple fashion the interfacial tension measurements and the bending elastic constants κ and $\overline{\kappa}$.

Since the pioneering work of Lang and Widom[20] it is

a)Author to whom correspondence should be addressed.
b)Permanent address: Institut für Physikalische Chemie, Universität zu Köln, Luxemburger Str. 116, D-50939 Köln, Germany.

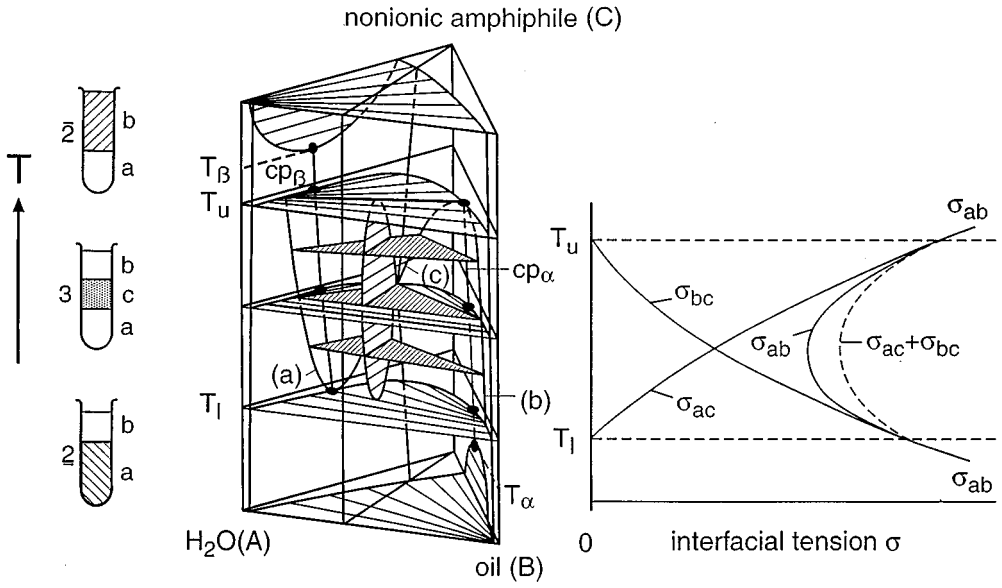

FIG. 1. Schematic phase prism of a water–oil–nonionic amphiphile (C_iE_j) system. The three test tubes on the left-hand side show the typical variation of the phase volumes. The microemulsion is shown hatched. The three interfacial tensions on the right-hand side illustrate the origin of the minimum of the water/oil interfacial tension σ_{ab} (Refs. 18 and 21).

known that $\underline{2}$, 3, $\overline{2}$ phase sequences are accompanied by interfacial tensions that may become ultralow. Interestingly, the interfacial tensions may become ultralow for various reasons. In all cases, however, the low values of the interfacial tensions are associated by a growing or even diverging length scale in the system.

Let us consider in Fig. 1 the typical phase behavior of nonionic microemulsions.[21,22]

Figure 1 demonstrates the $\underline{2}$, 3, $\overline{2}$ phase sequence and its link to the low interfacial tensions. With rising temperature, one observes that at T_l the lower phase microemulsion (lower test tube) splits into two phases, a and c. The lower water-rich phase (a) moves toward the water corner, while the surfactant-rich middle phase (c) moves toward the oil corner of the phase prism. At T_u, the upper phase microemulsion (upper test tube) is formed by the combination of the two phases c and b. Because for stability reasons[11]

$$\sigma_{ab} \leqslant \sigma_{ac} + \sigma_{bc}, \tag{1}$$

and $\sigma_{ac}+\sigma_{bc}$ runs through a minimum, σ_{ab} has to have a minimum as well. In order to sharpen the view for the relative shape of the individual curves, we redraw them using a logarithmic scale for the tensions and plot the independent variable temperature on the abszissa in Fig. 2.

All three interfacial tension curves have occasionally been determined in literature.[8,15,20] However, no systematic study has been performed on the location and shape of the σ_{ab}-curves, as they vary with oil and surfactant chain length. Such a study we present here. It is clear from Fig. 2 that, since σ_{ac} rises from zero at T_l and becomes identical with σ_{ab} at T_u, and since σ_{bc} rises from zero at T_u and becomes identical with σ_{ab} at T_l, the relative location of the individual σ_{ac}- and σ_{bc}-curves is fixed, if σ_{ab}, T_l and T_u are known. In the following we describe the experimental determination of these quantities for 19 different systems.

The present paper is organized as follows: In the theoretical section we recall well-known relations for interfacial tensions. We draw attention to the special situation when interfacial tensions become ultralow due to amphiphile adsorption. In the experimental section we describe the spinning-drop interfacial tension experiment, with emphasis on some indispensable precautions that we developed in order to minimize experimental errors. The interfacial tension

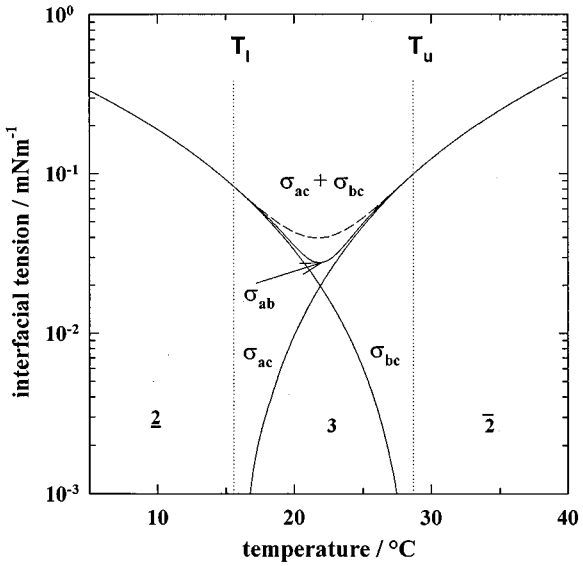

FIG. 2. Schematic shape of the individual interfacial tension curves, σ_{ab}, σ_{ac}, and σ_{bc} (on a log-scale) as a function of temperature.

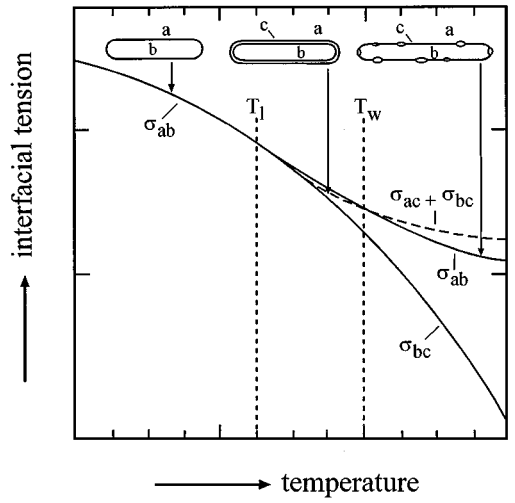

FIG. 3. Behavior of the interfacial tensions in the vicinity of the lower critical end point temperature T_l. For $T_l<T\leqslant T_w$ the middle phase (c) wets the macroscopic a/b interface, so that $\sigma_{ab}\geqslant\sigma_{ac}+\sigma_{bc}$. At the wetting temperature T_w, $\sigma_{ab}=\sigma_{ac}+\sigma_{bc}$, while for $T>T_w$ $\sigma_{ab}<\sigma_{ac}+\sigma_{bc}$. In addition the appearance of the cylindrical drop in the spinning-drop tension meter is shown schematically. Note that in the three-phase region the presence of the little c-phase blisters are essential for precise measurements.

data are given both in graphical and tabulated form. In the discussion section we perform a tentative evaluation in terms of bending elastic constants.

II. THEORETICAL CONSIDERATIONS

A microemulsion theory consistently explaining phase behavior, microstructure, and interfacial properties is still lacking.[23] If one is interested only in a semiquantitative understanding, one may note that microemulsions of length scale ξ are stable if

$$\sigma_{ab}\xi^2\cong kT, \tag{2}$$

where σ_{ab} is the macroscopic interfacial tension between the equilibrium microemulsion and the excess phase. If the microemulsion structure consists of droplets, the length scale ξ may be identified with the mean radius r of the droplets. In the case of three-phase coexistence, direct contact between water- and oil-rich excess phases is observable by removing most of the microemulsion middle phase (cf. Fig. 1). Then σ_{ab} refers to the interface between the water- and oil-rich excess phases, and ξ is to be identified with the domain size in the bicontinuous microemulsion. Equation (2) has been found to be a good first order description,[16,24–26] and may serve as a rule of thumb for semi-quantitative considerations.

A. Ultralow tensions approaching critical end points

When the three-phase regime is approached from the 2 phase state, for temperatures $T<T_l$, $\sigma_{ab}=\sigma_{bc}$. As the critical end point is reached, the water-rich microemulsion splits into two phases. Accordingly, the interfacial tension between them, σ_{ac}, starts from zero, and varies according to the scaling law $\sigma_{ac}=\sigma_{0,ac}\epsilon^{\mu}$, where $\mu=1.26$ is the critical exponent,[11,15] and $\epsilon=|T_l-T|/T_l$ is the distance from T_l. Very close to the critical end point the middle phase still wets the macroscopic a/b interface,[11] so that for $T_l<T\leqslant T_w$, $\sigma_{ab}\geqslant\sigma_{ac}+\sigma_{bc}$. At the wetting transition temperature T_w, $\sigma_{ab}=\sigma_{ac}+\sigma_{bc}$, while for $T>T_w$, $\sigma_{ab}<\sigma_{ac}+\sigma_{bc}$, and the interface between the water- and oil-rich excess phase is not wet by the middle phase. Figure 3 depicts such situation schematically.

In Fig. 3 we included also the appearance of the cylindrical drop in the tension meter. The presence of the little c-phase blisters on the cylindrical drop are essential for precise measurements in the three-phase region. In the wetting case the measurements are poorly reproducible and ill-defined. Such measurements are excluded from the present study. Experimentally, the gap between T_l and T_w is very small, 0.1 K or less for strong surfactants.[27,28] The analog sequence happens near the oil-rich critical end point at T_u.

B. Ultralow tensions approaching tricritical points

It is evident from Figs. 1 and 2 that by bringing T_l and T_u together, σ_{ab} can become very low. The close vicinity of both critical end points can be achieved by either approaching a tricritical point, at which the compositions of the critical end points become identical, or by increasing the efficiency of the surfactant. It has been shown in the past that in order to reach a tricritical point in these kinds of systems the structure has to be weakened.[23,27–30] This can be done by thermal energy, addition of a short-chain alcohol as cosolvent, a structure breaking salt, or a less hydrogen-bonding solvent. The other possibility is bringing T_u and T_l together by using strongly adsorbing amphiphiles.

C. Ultralow tensions due to amphiphile adsorption

The mean curvature H of the amphiphilic film is a monotonic function of, and changes dramatically with, temperature. It decreases almost linearly from large values at low temperatures (2), passes zero in the middle of the three-phase regime $T_m=(T_u+T_l)/2$, and becomes negative in the 2 state, that is to first order $H\approx c(T-T_m)$.[16] The temperature coefficient c is of the order of 10^{-3} Å^{-1}K^{-1} for all surfactants studied here, and decreases only slightly with increasing surfactant chain length, i (cf. Table II, below). Then

$$T_u-T_l\approx(H_l-H_u)/c, \tag{3}$$

where H_l and H_u are the mean curvature of the amphiphilic film at T_l and T_u. Note that $H_l\cong-H_u$. The approximate relation Eq. (3) permits rationalizing why an efficient (''good'') surfactant necessarily is associated with T_u and T_l being close together. Note that it is a general property of efficient surfactants to stabilize large structures (i.e., small $|H|$).

D. Scaling of the interfacial tensions

Based on the observed variation of the mean curvature with temperature, Strey[16] gave an empirical description of the interfacial tensions in the water–n-octane–$C_{12}E_5$ system in terms of bending elastic constants. Leitao *et al.*[19] realized

that the description could be generalized, and recently gave a scaling description of the interfacial tension curves for four systems. In this paper we show that the scaling relation is valid for all 19 systems studied up to now. While the reader is referred to the quoted papers for details, the equations for the reduced variables are repeated here. We define a reduced interfacial tension

$$\sigma^* = \sigma_{ab} / \overline{\sigma_{ab}}, \tag{4}$$

and temperature

$$\tau^* = \tau \sqrt{-\frac{2\kappa + \overline{\kappa}}{\overline{\kappa}}}, \tag{5}$$

where

$$\overline{\sigma_{ab}} = -\frac{\overline{\kappa}}{\overline{\xi^2}} \tag{6}$$

is the minimum interfacial tension, and

$$\overline{\xi} = \frac{2}{c(T_u - T_l)} \tag{7}$$

is the length scale at T_m. The temperature scale is reduced by the height of the three-phase interval $T_u - T_l$,

$$\tau = \frac{2(T - T_m)}{(T_u - T_l)}. \tag{8}$$

These quantities combine to give a very simple scaling relation

$$\sigma^* = (\tau^*)^2 + 1, \tag{9}$$

which is shown below to describe the data remarkably well. The two free parameters are the bending constant κ and the saddle-splay constant $\overline{\kappa}$. The other parameters are known from experimental determinations, T_u and T_l from the phase behavior, and $\overline{\xi}$ from scattering experiments.

III. EXPERIMENT

A. Materials

All *n*-alkanes used in this study were purchased from Merck or Aldrich with a purity $>99\%$. Water was bidistilled. The *n*-alkylpolyglycolethers, C_iE_j, were purchased from Bachem, Fluka, or Nikko with a purity $>98\%$. The solvents and the surfactants were used without further purification. To check the purity of the surfactants and to monitor any degradation, the cloud points at the critical compositions of the binary system's water–C_iE_j were always measured. Standard values provided by Schubert *et al.*[31,32] were used to judge the purity.

B. Sample preparation

For measuring the interfacial tension σ_{ab} macroscopic phase equilibrium was established. The samples typically contained equal volumes of water and oil, and depending on the efficiency of the surfactant, a surfactant concentration between 1.5 and 5 wt. %. The samples were prepared in a modified dropping funnel and equilibrated at the temperature to be examined. After complete phase separation, an extraction of the oil-rich phase is possible without disturbing the phase separation by using a syringe with a long needle from the top. The water-rich phase is extracted through the outlet at the bottom of the dropping funnel.

C. Density measurements

The densities of the coexisting phases were measured with a digital density meter (DMA 60, Anton Paar KG, Graz, Austria). The accuracy of the density measurements is essentially limited by the stability of the temperature control. With a compact low-temperature thermostat (RM 6, Lauda-Königshofen, Germany) a stability of 0.02 °C is reached. The accuracy of the density measurements is about $\pm 4 \cdot 10^{-5}$ g cm^{-3}.

D. Interfacial tension measurements

The ultralow interfacial tensions were measured using a spinning-drop tension meter (SITE 04, Krüss, Hamburg). This type of tension meter, developed by Cayias *et al.*[33] and subsequently modified by Burkowsky and Marx,[34] permits measuring interfacial tensions down to 10^{-5} m Nm^{-1}. It consists of a thermostatable horizontal glass capillary rotating about its long axis with a maximum speed of 10 000 rpm. In our study the tension meter was modified for small sample volumes. For this purpose two septa (soft polyethylene discs) are used for sealing the glass capillary. Two syringes equipped with acute needles, one for injecting and one for taking up the overflow, are stuck into the respective ends of the capillary. Importantly, the syringe holder on the inlet side was modified to be thermostated. In this fashion, phase separation could be avoided.

For measuring the interfacial tension σ_{ab}, the capillary was filled using a 2 ml syringe, taking care that no air bubbles entered the inlet side. At a relatively slow speed of rotation of 1000 rpm, 2 ml of the thermostated water-rich phase were pushed through the capillary and into the outlet syringe with about 1 ml of the phase remaining in the capillary. Hereafter the rotation of the capillary was interrupted in order to inject the oil-rich phase with a μl-syringe (Hamilton) through the inlet side. The injected volume of the oil-rich phase varied between 0.2 and 3 μl, depending on the expected interfacial tension. Subsequently, the rotation of the capillary was restarted in order to center the injected oil-rich drop. To this end the capillary was tilted, letting the drop slowly move toward the center of the viewing field of the microscope. There its diameter was measured.

It is important to realize that during the filling of the capillary, problems arise because of temperature gradients during the transfer of both the water- and the oil-rich phases. Both phases may phase separate, a process which is irreversible inside the capillary. For this reason, thermostating the syringe holder on the inlet side is indispensable. By means of this detachable, thermostatable syringe holder, the preequilibrated phases could be transferred without phase separation. This modification allows for sufficiently stable, and

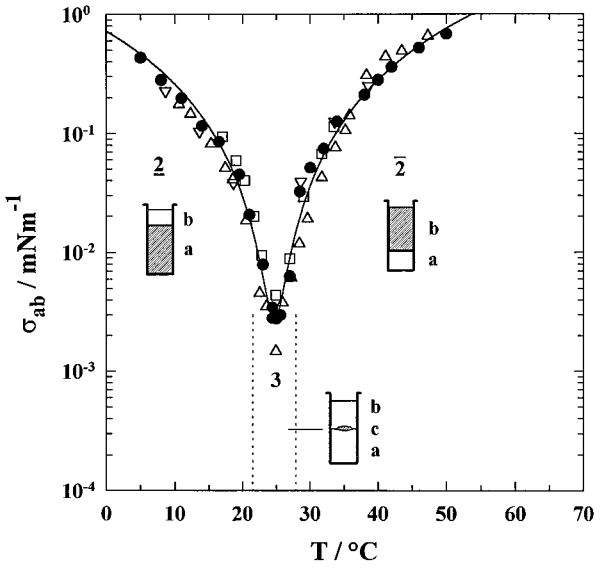

FIG. 4. Interfacial tensions σ_{ab} (circles) in the water–*n*-octane–$C_{10}E_4$ system as function of temperature. Data obtained by Fletcher *et al.* (Ref. 13) (triangles) and Kahlweit *et al.* (Ref. 26) (reversed triangles) with the spinning drop, and by Langevin *et al.* (Ref. 36) (squares) with surface light scattering are shown for comparison. The full line drawn to guide the eye is calculated from the interfacial tension model (Refs. 16 and 19). The test tubes illustrate which interface the measurement refers to.

homogenous, drops of the oil-rich phase, which by increasing speed of rotation deform into well-shaped cylinders.

In the three-phase region an additional problem arises in the form of an instability and permanent increase of the drop diameter. The increase of the drop diameter was found to be caused by an increasing lack of surfactant molecules in the drop. Apparently, the molecules enrich on heterogeneous surfaces (i.e., the walls of the capillary or dust particles) due to their interfacial activity. This problem could be remedied by enriching the oil-rich phase with minute traces of surfactant. In a series of experiments it was found that such enrichment leads to the formation of the third phase, as is to be expected from the phase behavior.[21] The third phase appears in the form of small blisters on the surface of the cylindrical drop. As long as the surface area covered by the small blisters is below 10% of the total cylinder area, the interfacial tension stays exactly constant.

The procedure described permits measurements of the drop diameter, and thus of the interfacial tension, over a temperature range from 0 to 70 °C without great difficulties. The interfacial tensions were calculated from Vonnegut's[35] equation. He considered the drop as a cylinder of radius r and length l with hemispherical ends. For drops of $l \gg r$, the interfacial tension could be evaluated by

$$\sigma = \tfrac{1}{4}(\rho_1 - \rho_2)\omega^2 r^3, \tag{10}$$

where ω is the angular velocity and $(\rho_1 - \rho_2)$ is the density difference of the two phases. In practice, speeds of rotation between 2500 and 5500 rpm were used. The radius is obtained by measuring the diameter of the cylindrical drop through the eye piece of a microscope. The grating visible in the eye piece is calibrated by comparison to the known diameter of a straight, thin wire.

E. Measuring accuracy and errors

The interfacial tensions in this study are, in general, averages of at least 20 single measurements. The error of the single measurement depends on the magnitude of the interfacial tension. It ranges between $\pm 5\%$ and $\pm 30\%$ for tensions of 1 and 10^{-4} m Nm^{-1}, respectively. Systematic errors may occur due to improper handling of the surfactant. Degradation will shift the phase behavior on the temperature scale. Insufficient equilibration outside or inside the measurement cell is another source of uncertainty.

IV. RESULTS

The primary results are interfacial tensions σ_{ab} ranging over several orders of magnitude as a function of temperature. In the graphical representations of the data the same scale will be used for all data. In this fashion a quantitative comparison is possible. The experiments cover the range $0.0001 < \sigma_{ab}/\text{m Nm}^{-1} < 1$ and $0 < T/°\text{C} < 70$. The hydrocarbon chain length of the oil, k, the head group, j, and the hydrocarbon tail length, i, of the surfactants was varied. The numerical values of the interfacial tensions along with the temperature of measurement are compiled in Table I.

Also given is the phase state p, 2, 3, or 2̄, indicating in which regime the measurement was carried out.

A. Comparison with literature data

In Fig. 4 a comparison with literature data is performed.[13,26,36] The experimental error of our data amounts to about a symbol width. As is evident, the data fall on a smooth curve irrespective of whether they are measured in the 2, 3, or 2̄ regime. The test tubes illustrate the respective states. The solid line is the theoretical description following below. It should be viewed as a guide to the eye at this stage.

B. Variation of oil chain length, *k*

In Fig. 5 the interfacial tensions for C_8E_3, $C_{10}E_4$, and $C_{12}E_5$ are shown for $k=8$ to 14. As can be seen, for each surfactant the minima shift to higher temperature, as do the three-phase bodies.[22] The minima become more shallow, in correspondence to the increasing width $T_u - T_l$ of the three-phase bodies. With increasing oil chain length from $k=8$ to 14, the minima increase by an order of magnitude. With increasing surfactant size the minimum tensions become very much lower.

C. Variation of the head group size, *j*

The interfacial tensions for the C_8E_j series with $j=3,4,5$ and octane as oil are shown on the left in Fig. 6. While the shift of the minimum tensions follows the shift of three-phase bodies on the temperature scale, the absolute value of the interfacial tension at the minimum increases slightly. A somewhat surprising result, if one considers that the molecular length of the amphiphile increases. The

TABLE I. The numerical values of the oil–water interfacial tension σ_{ab} is given along with the measurement temperature and the phase state p, indicating in which regime the measurement was carried out.

p	T/°C	σ_{ab} /m Nm^{-1}	p	T/°C	σ_{ab} /m Nm^{-1}	p	T/°C	σ_{ab} /m Nm^{-1}	p	T/°C	σ_{ab} /m Nm^{-1}	p	T/°C	σ_{ab} /m Nm^{-1}	p	T/°C	σ_{ab} /m Nm^{-1}
	H_2O-n-C_8H_{18}-C_6E_2		$\underline{3}$	28.0	9.1×10^{-2}	3	55.0	1.2×10^{-1}		H_2O-n-$C_{12}H_{26}$-$C_{10}E_4$		3	64.0	2.1×10^{-2}	$\underline{3}$	40.5	2.8×10^{-3}
3	1.0	1.3×10^{-1}	$\underline{2}$	29.0	1.1×10^{-1}	3	58.0	7.6×10^{-2}	$\underline{2}$	20.0	2.2×10^{-1}	3	64.1	1.9×10^{-2}	$\underline{2}$	43.0	1.9×10^{-2}
3	4.5	9.9×10^{-2}	$\underline{2}$	32.5	1.9×10^{-1}	3	61.0	6.3×10^{-2}	$\underline{2}$	28.0	7.1×10^{-2}	3	65.5	3.0×10^{-2}	$\underline{2}$	46.0	5.3×10^{-2}
3	7.4	8.3×10^{-2}	2	34.0	2.3×10^{-1}	3	62.0	5.9×10^{-2}	3	32.0	2.3×10^{-2}				2	50.0	1.2×10^{-1}
$\underline{3}$	10.0	1.1×10^{-1}				3	63.0	4.6×10^{-2}	3	33.5	1.6×10^{-2}		H_2O-n-C_8H_{18}-$C_{12}E_4$				
$\underline{2}$	15.0	2.1×10^{-1}		H_2O-n-$C_{12}H_{26}$-C_8E_3		3	65.0	6.0×10^{-2}	3	35.6	1.1×10^{-2}	$\underline{2}$	7.4	4.3×10^{-2}		H_2O-n-$C_{12}H_{26}$-$C_{12}E_5$	
$\underline{2}$	20.0	3.7×10^{-1}	$\underline{2}$	17.0	1.6×10^{-1}	3	66.5	9.7×10^{-2}	3	37.5	1.4×10^{-2}	$\underline{2}$	9.4	1.8×10^{-2}	$\underline{2}$	30.0	1.3×10^{-1}
$\underline{2}$	25.0	6.5×10^{-1}	$\underline{2}$	18.0	2.0×10^{-1}	3	68.0	1.3×10^{-1}	$\underline{3}$	39.0	2.6×10^{-2}	$\underline{3}$	12.2	9×10^{-4}	$\underline{2}$	33.0	7.7×10^{-2}
$\underline{2}$	30.0	1.0	3	21.0	9.9×10^{-2}				$\underline{2}$	43.0	7.5×10^{-2}	$\underline{2}$	14.4	3.1×10^{-3}	$\underline{2}$	36.0	5.6×10^{-2}
$\underline{2}$	35.0	1.4	3	25.0	6.7×10^{-2}		H_2O-n-C_8H_{18}-$C_{10}E_4$		2	50.0	2.2×10^{-1}	$\underline{2}$	15.7	5.9×10^{-3}	$\underline{2}$	39.0	2.5×10^{-2}
$\underline{2}$	40.0	1.9	3	26.5	4.5×10^{-2}	$\underline{2}$	5.0	4.3×10^{-1}				$\underline{2}$	16.4	1.2×10^{-2}	3	43.0	3.0×10^{-3}
$\underline{2}$	45.0	2.2	3	28.0	4.8×10^{-2}	$\underline{2}$	8.0	2.8×10^{-1}		H_2O-n-$C_{14}H_{30}$-$C_{10}E_4$		$\underline{2}$	17.7	2.7×10^{-2}	3	44.0	2.3×10^{-3}
$\underline{2}$	50.0	2.8	3	29.4	4.9×10^{-2}	$\underline{2}$	11.0	2.0×10^{-1}	$\underline{2}$	28.0	1.3×10^{-1}	$\underline{2}$	19.4	4.1×10^{-2}	$\underline{3}$	45.5	6.8×10^{-3}
2	55.0	3.2	3	31.0	6.7×10^{-2}	$\underline{2}$	14.0	1.2×10^{-1}	$\underline{2}$	32.0	7.5×10^{-2}	2	19.7	6.8×10^{-2}	$\underline{2}$	49.0	3.2×10^{-2}
			$\underline{3}$	36.0	1.7×10^{-1}	$\underline{2}$	16.5	8.5×10^{-2}	3	37.0	2.7×10^{-2}				2	53.0	8.5×10^{-2}
	H_2O-n-C_8H_{18}-C_8E_3		2	39.0	2.1×10^{-1}	$\underline{2}$	19.5	4.5×10^{-2}	3	38.5	2.4×10^{-2}		H_2O-n-C_8H_{18}-$C_{12}E_5$				
$\underline{2}$	7.0	1.3×10^{-1}				$\underline{2}$	21.0	2.1×10^{-2}	3	40.0	2.0×10^{-2}	$\underline{2}$	10.25	4.1×10^{-1}		H_2O-n-$C_{14}H_{30}$-$C_{12}E_5$	
$\underline{2}$	10.0	8.5×10^{-2}		H_2O-n-$C_{14}H_{30}$-C_8E_3		3	23.0	7.9×10^{-3}	3	41.5	2.3×10^{-2}	$\underline{2}$	16.05	2.2×10^{-1}	$\underline{2}$	38.0	1.1×10^{-1}
3	14.3	2.6×10^{-2}	3	23.0	1.9×10^{-1}	3	24.4	3.1×10^{-3}	3	43.5	2.8×10^{-2}	$\underline{2}$	20.55	1.1×10^{-1}	$\underline{2}$	40.5	6.3×10^{-2}
3	15.8	1.5×10^{-2}	3	28.0	1.3×10^{-1}	3	25.0	2.8×10^{-3}	$\underline{3}$	48.0	9.2×10^{-2}	$\underline{2}$	24.25	6.4×10^{-2}	$\underline{2}$	42.5	3.9×10^{-2}
3	16.5	1.6×10^{-2}	3	32.0	1.1×10^{-1}	3	25.6	3.0×10^{-3}	2	52.0	1.5×10^{-1}	$\underline{2}$	25.25	$4.3\times^{-2}$	3	47.5	7.2×10^{-3}
3	17.3	1.9×10^{-2}	3	33.6	1.0×10^{-1}	$\underline{3}$	27.0	6.3×10^{-3}				$\underline{2}$	28.25	1.9×10^{-2}	3	49.0	4.7×10^{-3}
$\underline{3}$	19.0	3.6×10^{-2}	3	35.0	1.1×10^{-1}	$\underline{2}$	28.5	3.2×10^{-2}		H_2O-n-C_8H_{18}-$C_{10}E_5$		3	32.15	2.7×10^{-3}	$\underline{3}$	50.5	7.1×10^{-3}
$\underline{2}$	22.0	8.7×10^{-2}	$\underline{3}$	38.0	1.2×10^{-1}	$\underline{2}$	30.0	5.1×10^{-2}	$\underline{2}$	30.0	2.2×10^{-1}	3	32.85	5×10^{-4}	$\underline{2}$	55.5	6.6×10^{-2}
$\underline{2}$	25.0	1.4×10^{-1}	2	45.0	3.0×10^{-1}	$\underline{2}$	32.0	7.4×10^{-2}	$\underline{2}$	35.0	1.1×10^{-1}	3	33.25	8×10^{-4}	2	57.0	8.1×10^{-2}
$\underline{2}$	30.0	2.6×10^{-1}				$\underline{2}$	34.0	1.3×10^{-1}	$\underline{2}$	39.0	3.9×10^{-2}	$\underline{3}$	33.35	1.1×10^{-3}			
$\underline{2}$	35.0	4.0×10^{-1}		H_2O-n-C_8H_{18}-C_8E_4		$\underline{2}$	38.0	2.1×10^{-1}	3	43.5	1.0×10^{-2}	$\underline{2}$	36.25	1.5×10^{-2}		H_2O-n-C_8H_{18}-$C_{12}E_6$	
$\underline{2}$	40.0	6.6×10^{-1}	$\underline{2}$	27.0	2.6×10^{-1}	$\underline{2}$	40.0	2.8×10^{-1}	3	45.5	4.9×10^{-3}	$\underline{2}$	38.25	3.4×10^{-2}	$\underline{2}$	40.0	6.8×10^{-2}
$\underline{2}$	45.0	9.3×10^{-1}	$\underline{2}$	30.0	1.9×10^{-1}	$\underline{2}$	42.0	3.6×10^{-1}	$\underline{3}$	46.5	1.0×10^{-2}	$\underline{2}$	40.25	5.3×10^{-2}	$\underline{2}$	43.0	3.3×10^{-2}
$\underline{2}$	50.0	1.2	$\underline{2}$	35.0	7.9×10^{-2}	$\underline{2}$	46.0	5.2×10^{-1}	$\underline{2}$	50.0	6.1×10^{-2}	$\underline{2}$	43.25	1.3×10^{-1}	$\underline{2}$	45.0	1.4×10^{-2}
$\underline{2}$	55.0	1.6	3	40.0	4.4×10^{-2}	2	50.0	6.7×10^{-1}	$\underline{2}$	54.0	1.2×10^{-1}	$\underline{2}$	47.25	2.3×10^{-1}	3	47.5	2.0×10^{-3}
2	60.0	2.2	3	41.7	2.8×10^{-2}				2	58.0	2.4×10^{-1}	$\underline{2}$	50.25	3.1×10^{-1}	3	48.0	2.8×10^{-3}
			3	42.5	3.1×10^{-2}		H_2O-n-$C_{10}H_{22}$-$C_{10}E_4$					2	54.25	4.3×10^{-1}	3	48.4	1.8×10^{-3}
	H_2O-n-$C_{10}H_{22}$-C_8E_3		$\underline{3}$	43.4	4.4×10^{-2}	$\underline{2}$	20.0	1.0×10^{-1}		H_2O-n-C_8H_{18}-$C_{10}E_6$					$\underline{3}$	49.5	3.2×10^{-3}
$\underline{2}$	10.0	1.9×10^{-1}	$\underline{2}$	50.0	1.5×10^{-1}	$\underline{2}$	26.0	3.0×10^{-2}	$\underline{2}$	46.5	2.5×10^{-1}		H_2O-n-$C_{10}H_{22}$-$C_{12}E_5$		$\underline{2}$	53.0	2.6×10^{-2}
$\underline{2}$	15.0	8.4×10^{-2}	2	57.0	3.9×10^{-1}	3	29.0	1.1×10^{-2}	$\underline{2}$	51.5	1.2×10^{-1}	$\underline{2}$	28.0	1.1×10^{-1}	2	55.0	5.0×10^{-2}
3	18.0	5.4×10^{-2}				3	30.5	5.9×10^{-3}	3	56.5	4.9×10^{-2}	$\underline{2}$	31.5	4.5×10^{-2}			
3	20.0	3.5×10^{-2}		H_2O-n-C_8H_{18}-C_8E_5		$\underline{3}$	32.0	8.4×10^{-3}	3	58.0	4.2×10^{-2}	$\underline{2}$	34.0	2.8×10^{-2}			
3	22.1	3.3×10^{-2}	$\underline{2}$	44.0	4.1×10^{-1}	$\underline{2}$	35.0	3.4×10^{-2}	3	60.5	1.4×10^{-2}	3	38.6	1.3×10^{-3}			
3	24.0	4.3×10^{-2}	$\underline{2}$	51.0	1.8×10^{-1}	2	42.0	1.6×10^{-1}	3	61.5	1.2×10^{-2}	3	39.4	9×10^{-4}			

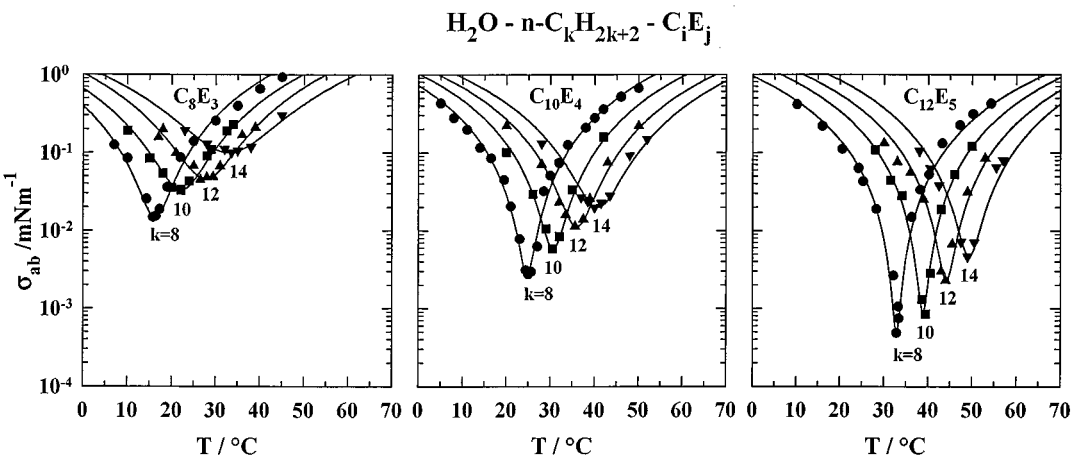

FIG. 5. Variation of the interfacial tension curves as a function of the oil chain length k for the C_8E_3, $C_{10}E_4$, and $C_{12}E_5$-systems. Note that for each system the minimum of the curves increases with increasing k and shifts to a higher temperature.

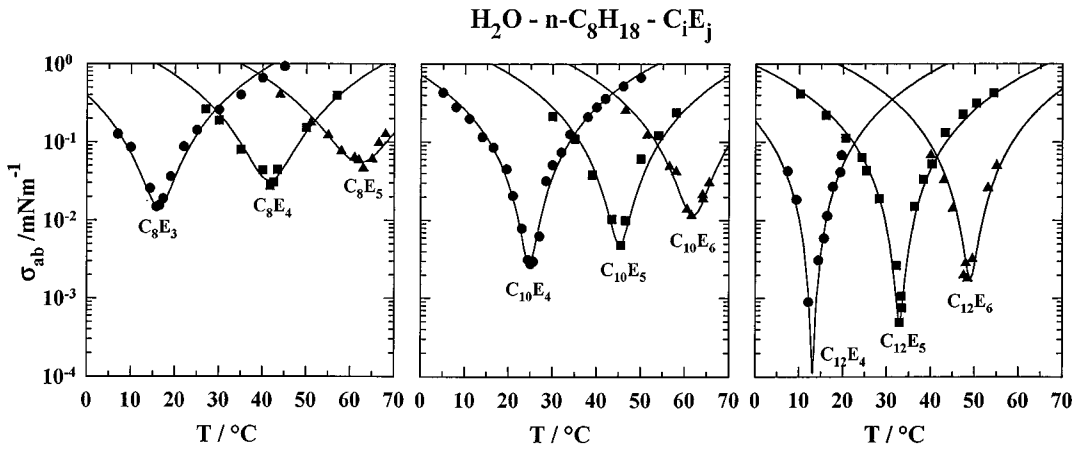

FIG. 6. Variation of the interfacial tension curves as a function of the head group size j for the C_8E_j, $C_{10}E_j$ and $C_{12}E_j$-series and octane as oil. Note that for each series the minimum of the curves increases slightly with increasing j.

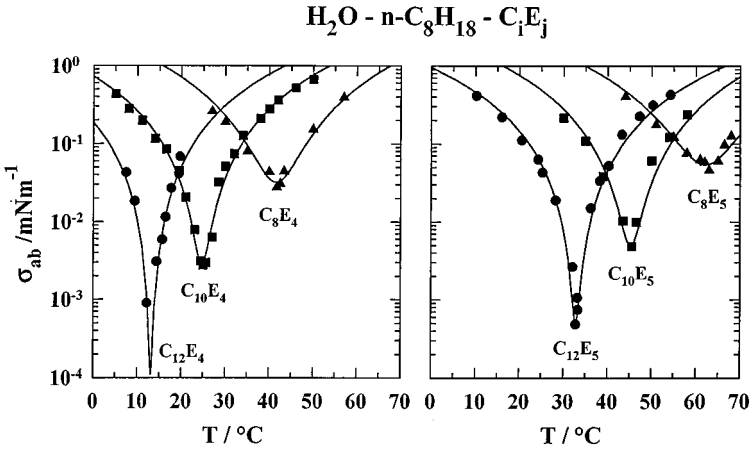

FIG. 7. Variation of the interfacial tension curves as a function of the surfactant chain length i for the C_iE_4 and C_iE_5-series and octane as oil. Note that for each series the minimum of the curves decreases strongly with increasing i and shifts to a lower temperature.

$C_{10}E_j$ series, presented in Fig. 6, center, with $j=4,5,6$ shows the same trends as the C_8E_j. However, the increase in the hydrophobic chain leads to an overall lowering of the interfacial tensions by an order of magnitude. The $C_{12}E_j$ series, with $j=4,5,6$, finally shows lower tensions again by another order of magnitude (Fig. 6, right).

D. Variation of surfactant chain length, *i*

While already implicitly present in Figs. 5 and 6, the comparatively strong chain length dependence is borne out for C_iE_4 and C_iE_5 with $i=8,10,12$ in Fig. 7. This comparison also illustrates the increasing deepness of the V-shaped curves with increasing i.

V. INTERPRETATION AND DISCUSSION

Systematic trends in the variations of the interfacial tensions with i, j, and k are observed. The interpretation of the actual numerical values and their variation with temperature is not trivial and presumably not unique. For that reason we have given the numerical values in Table I to be used by other workers.

In the following, we present a tentative interpretation based on bending energy considerations.[16,19,37] As we showed in a previous paper,[16] the minimum of the tension curves is associated with the mean curvature of the amphiphilic film in the microemulsions passing through zero. The minima and passing through zero are qualitatively similar both for long- and short-chain surfactants. Langevin and co-workers[36] have shown that the persistence length of short-chain surfactants is smaller than that of long-chain surfactants. The idea, originally expressed by De Gennes and Taupin,[5] is that the long-chain surfactants are able to solubilize more of the solvents due to the increased rigidity. This in turn leads to longer length scales in the microemulsions. Before we turn to the scaling of the tensions, let us consider the original expression for the interfacial tension based on simple bending energy arguments,[16,19]

$$\sigma_{ab}=-\frac{\overline{\kappa}(T_u-T_l)^2c^2}{4}\left\{-\frac{2\kappa+\overline{\kappa}}{\overline{\kappa}}\left[\frac{2(T-T_m)}{T_u-T_l}\right]^2+1\right\}. \tag{11}$$

After measuring $\overline{\xi}$ by SANS[38] and determining c according to Eq. (7), Eq. (11) contains only two free parameters, κ and $\overline{\kappa}$. For $T=T_m$, $\overline{\kappa}$ is directly obtained from the minimum of the interfacial tensions. κ is then determined by adjusting the opening angles of the V-shaped interfacial tension curves. The necessary parameters from auxiliary measurements T_u, T_l, and $\overline{\xi}$ are given in Table II. In the procedure of fitting each σ_{ab} curve, the bending elastic constants for each system are obtained. These are also given in Table II.

Since all interfacial tension curves follow the same functional form, one may try to scale them. This is done by the procedure discussed in the theoretical section. The result is shown in Fig. 8. The solid line is calculated from Eq. (9), and it describes the data within experimental error. Figure 8 is an extension and confirmation of our previous findings[16,19] for a few selected systems.

The interesting question is, what are the trends of the elastic constants? The variation of the elastic constants with the maximum length scale $\overline{\xi}$ is shown in Fig. 9. The bending constant κ ranges between 0.59 and 1.3 kT, while the saddle-splay constant $\overline{\kappa}$ ranges between -0.31 and -0.7 kT. Building the average ratio over all systems (excluding the highest and lowest values), we find

$$\kappa=-2.06\overline{\kappa}. \tag{12}$$

Including all data, the prefactor in Eq. (12) becomes 2.14. For liquid films one would expect[39] $\kappa=-2\overline{\kappa}$.

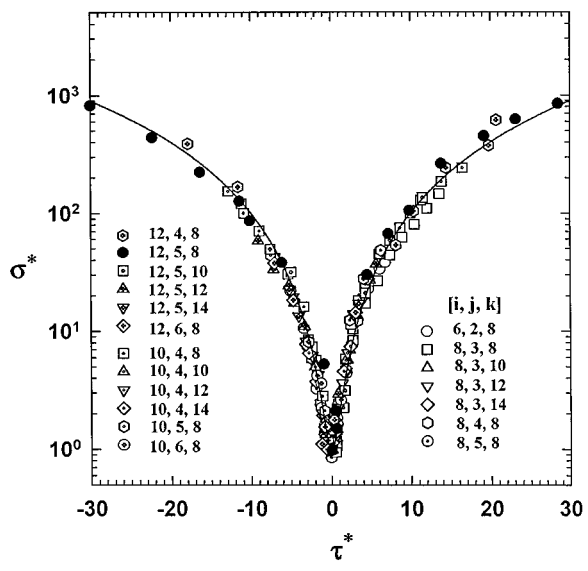

FIG. 8. Reduced oil–water interfacial tension σ^* as a function of reduced temperature τ^* (see text for definitions) for all 19 systems. The full line is calculated from $\sigma^*=(\tau^*)^2+1$.

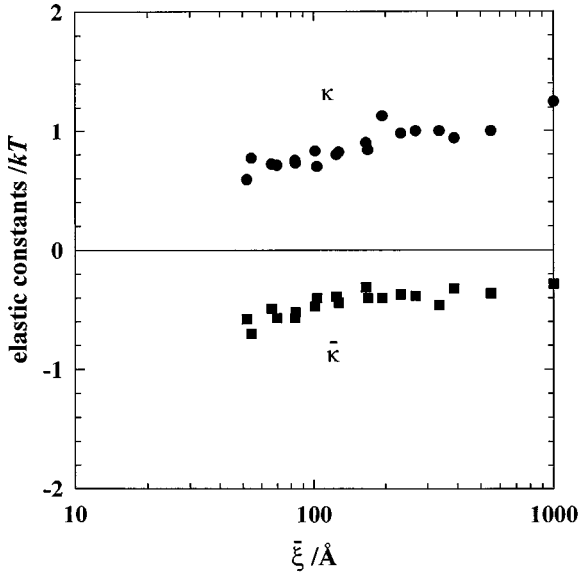

FIG. 9. Variation of the elastic parameters κ and $\overline{\kappa}$ as a function of the maximum length scale $\overline{\xi}$. Note that with increasing $\overline{\xi}$ the bending constant κ increases, while the absolute value of the saddle-splay constant $\overline{\kappa}$ decreases.

TABLE II. The systems are characterized by the surfactant chain length i, the head group size j, and the oil chain length k. For each system the upper and lower critical end point temperatures, T_u and T_l, the experimental value of the oil–water interfacial tension at the minimum, $\overline{\sigma_{ab}}$, the maximum length scale, ξ, the temperature coefficient of the mean curvature, c, and the elastic parameters, κ and $\overline{\kappa}$, are given.

i	j	k	T_l/°C	T_u/°C	$\overline{\sigma_{ab}}$/m Nm^{-1}	$\overline{\xi}$/Å	c/(Å K)$^{-1}$	κ/kT	$\overline{\kappa}/kT$
6	2	8	−0.80	13.65	0.0830	51.9	0.0027	0.59	−0.58
8	3	8	11.17	21.32	0.0149	103	0.0019	0.70	−0.40
8	3	10	15.58	28.68	0.0332	83.2	0.0018	0.75	−0.57
8	3	12	19.40	36.08	0.0460	66.1	0.0018	0.72	−0.49
8	3	14	22.50	43.40	0.1000	54.3	0.0018	0.77	−0.70
8	4	8	35.25	47.95	0.0320	83.5	0.0019	0.73	−0.52
8	5	8	54.30	70.12	0.0540	69.7	0.0018	0.71	−0.57
10	4	8	21.50	27.90	0.0028	231	0.0014	0.98	−0.37
10	4	10	26.50	34.82	0.0059	168	0.0014	0.84	−0.40
10	4	12	30.43	41.65	0.0114	127	0.0014	0.82	−0.44
10	4	14	33.50	48.05	0.0201	101	0.0014	0.83	−0.47
10	5	8	40.75	49.75	0.0049	165	0.0013	0.90	−0.31
10	6	8	56.50	67.22	0.0116	124	0.0015	0.80	−0.39
12	4	8	12.20	14.00	(0.00011)	(1000)	0.0011	1.25	−0.28
12	5	8	31.25	34.45	0.0005	550	0.0011	1.00	−0.36
12	5	10	36.67	41.00	0.0009	387	0.0012	0.94	−0.32
12	5	12	40.95	47.40	0.0023	267	0.0012	1.00	−0.38
12	5	14	44.60	54.10	0.0047	193	0.0011	1.13	−0.40
12	6	8	46.68	51.40	0.0018	335	0.0013	1.00	−0.46

A number of difficult to answer questions arise. What is the nature of the elastic constants deduced (bare or renormalized, i.e., length scale dependent)?[36] How to take renormalization, translational entropy, entropy of fluctuations, and polydispersity into account? A theoretical treatment of the seemingly simple droplet case has recently been given by Palmer and Morse.[40] In our tentative interpretation we have made a number of simplifying assumptions, and we have neglected entropy considerations. It is still surprising that such a simple description seems to suffice.

Recently Gradzielski *et al.*[41,42] found, by analyzing SANS and interfacial tension measurements for droplet microemulsions in terms of bending elastic constants for the sum $2\kappa+\overline{\kappa}$, comparable, but slightly larger values due to inclusion of a translational entropy term.

One might wonder how closely the rule of thumb in Eq. (2) is valid. According to Eq. (6) $-\overline{\kappa}=\overline{\sigma_{ab}}\overline{\xi^2}$. Building the average value for all systems examined one finds $0.44kT$ with a standard deviation of 0.10. This means that the rule of thumb [Eq. (2)] is not only fulfilled to the order of magnitude, but almost within a factor of 2.

Another observation possibly deserves attention. In critical phenomena, scaling descriptions have been *en vogue* for the last 30 years. In near-critical systems a universal ratio R has been found from the critical scaling laws,[43,44] with experiments and theory now agreeing that[44–46]

$$R=\sigma_0\xi_0^2=0.37(\pm 0.03)kT. \tag{13}$$

We wonder whether there is a deeper meaning to the coincidence of R with the numerical value of $\overline{\sigma_{ab}}\overline{\xi^2}=0.44$ (± 0.10) kT. The significance of this observation remains to be understood.

VI. CONCLUSIONS

The simple description of interfacial tensions over the whole temperature range by an analytical form suggested previously[16] is shown to be valid for all 19 systems. From the analysis the bending constants κ and $\overline{\kappa}$ are obtained. The measured data points are described within experimental error. The scaling version of this description recently suggested[19] needs the upper and lower critical end point temperature, and the maximum length scale for the symmetrical microemulsion as input data. All these parameters have been determined. Plotting the reduced interfacial tension σ^* against a reduced temperature τ^*, all data fall on the simple master curve given by $\sigma^*=(\tau^*)^2+1$.

ACKNOWLEDGMENTS

Part of the measurements were performed in the department of Professor M. Kahlweit. We are indebted to him for supporting the work. We also thank T. Lieu for assistance with the interfacial measurements. Also acknowledged is fruitful interaction with D. Langevin and M. M. Telo da Gama within the frame of the program ''Human Capital and Mobility'' (ERB4001GT931413).

[1] P. A. Winsor, *Solvent Properties of Amphiphilic Compounds* (Butterworth, London, 1954); P. A. Winsor, Chem. Rev. **68**, 1 (1968).
[2] J. H. Schulman and J. B. Montagne, Ann. N. Y. Acad. Sci. **92**, 366 (1961).
[3] L. M. Prince, *Microemulsions* (Academic, New York, 1977).
[4] M. L. Robbins, in ''Micellization,'' *Solubilization, and Microemulsions*, edited by K. W. Mittal (Plenum, New York, 1977), p. 713.
[5] P. G. De Gennes and C. Taupin, J. Phys. Chem. **86**, 2294 (1982).
[6] A. Ben-Shaul, L. Szleifer, and W. M. Gelbart, in *Physics of Amphiphiles*, edited by D. Langevin, J. Meunier, and N. Boccara (Springer, New York, 1987), p. 2.
[7] W. Helfrich, Z. Naturforsch. **28C**, 693 (1973).

[8] A. Cazabat, D. Langevin, J. Meunier, and A. Pouchelon, J. Phys. Lett. **43**, (1982).
[9] H. Kunieda and K. Shinoda, J. Colloid Interface Sci. **107**, 107 (1985).
[10] R. S. Schechter, W. H. Wade, U. Weerasooriya, V. Weerasooriya, and S. Yiv, J. Dispers, Sci. Techn. **6**, 223 (1985).
[11] B. Widom, Langmuir **3**, 12 (1987).
[12] R. Aveyard, B. P. Binks, and P. D. I. Fletcher, Langmuir **5**, 1210 (1989).
[13] D. I. Fletcher and D. I. Horsup, J. Chem. Soc. Faraday Trans. **88**, 855 (1992).
[14] M. Kahlweit, R. Strey, D. Haase, and P. Firman, Langmuir **4**, 785 (1988).
[15] K. Bonkhoff, A. Hirtz, and G. H. Findenegg, Physica A **172**, 174 (1991).
[16] R. Strey, Colloid Polym. Sci. **272**, 1005 (1994).
[17] T. Sottmann and R. Strey, J. Phys.: Condens. Matter **8**, A39 (1996).
[18] T. Sottmann and R. Strey, Ber. Bunsenges. Phys. Chem. **100**, 237 (1996).
[19] H. Leitao, A. M. Somoza, M. M. Telo da Gama, T. Sottmann, and R. Strey, J. Chem. Phys. **105**, 2875 (1996).
[20] J. C. Lang and B. Widom, Physica **81**A, 190 (1975).
[21] M. Kahlweit and R. Strey, Angew. Chem. Int. Ed. Engl. **24**, 654 (1985).
[22] M. Kahlweit, R. Strey, and P. Firman, J. Phys. Chem. **90**, 671 (1986).
[23] G. Gompper and M. Schick, *Self-Assembling Amphiphilic Systems* (Academic, New York, 1994).
[24] B. P. Binks, J. Meunier, O. Abillon, and D. Langevin, Langmuir **5**, 415 (1989).
[25] L. T. Lee, D. Langevin, J. Meunier, K. Wong, and B. Cabane, Prog. Colloid Polym. Sci. **81**, 209 (1990).
[26] M. Kahlweit, J. Jen, and G. Busse, J. Chem. Phys. **97**, 6917 (1992).
[27] M. Kahlweit, R. Strey, and G. Busse, Phys. Rev. **47**, 4197 (1993).
[28] K.-V. Schubert, R. Strey, S. R. Kline, and E. W. Kaler, J. Chem. Phys. **101**, 5343 (1994).
[29] M. Kahlweit, R. Strey, M. Aratono, G. Busse, J. Jen, and K.-V. Schubert, J. Chem. Phys. **95**, 2842 (1991).
[30] K.-V. Schubert and R. Strey, J. Chem. Phys. **95**, 8532 (1991).
[31] K.-V. Schubert, R. Strey, and M. Kahlweit, J. Colloid Interface Sci. **141**, 21 (1991).
[32] K.-V. Schubert, R. Strey, and M. Kahlweit, Prog. Colloid Polym. Sci. **84**, 103 (1991).
[33] J. L. Cayias, R. S. Schechter, and W. H. Wade, in *Adsorption at Interfaces*, edited by K. L. Mittal, ACS Symposium Series Vol. 8, (ACS, Washington, DC, 1975).
[34] M. Burkowsky and C. Marx, Tenside Deterg. **5**, 247 (1978).
[35] B. Vonnegut, Rev. Sci. Instrum. **13**, 6 (1942).
[36] D. Langevin, in *Structure and Dynamics of Strongly Interacting Colloids and Supramolecular Aggregates in Solution*, edited by S.-H. Chen *et al.* (Kluwer, Dordrecht, 1992), p. 325.
[37] S. Safran, in *Structure and Dynamics of Strongly Interacting Colloids and Supramolecular Aggregates in Solution*, edited by S.-H. Chen *et al.* (Kluwer, Dordrecht, 1992), p. 237.
[38] T. Sottmann, R. Strey and S.-H. Chen, J. Chem. Phys. **106**, 6483 (1997).
[39] C. Varea and A. Robledo, Physica A **33**, 220 (1995).
[40] K. Palmer and D. C. Morse, J. Chem. Phys. **105**, 11147, 1996.
[41] M. Gradzielski, D. Langevin, and B. Farago, Phys. Rev. E **53**, 3900 (1996).
[42] M. Gradzielski, D. Langevin, T. Sottmann, and R. Strey, J. Chem. Phys. (in press).
[43] B. Widom, J. Chem. Phys. **43**, 3892 (1964).
[44] M. R. Moldover, Phys. Rev. A **31**, 1022 (1985).
[45] K. H. Mon, Phys. Rev. Lett. **60**, 2749 (1988).
[46] J. P. Rakotoniaina, L. Belkoura, and D. Woermann, Z. Phys. Chem. **196**, 237 (1996).